流体圧送による土壌層の破壊

誌名	専修大学北海道短期大学紀要
ISSN	02872838
著者名	新家,憲司 高,鋭
発行元	専修大学北海道短期大学
巻/号	17号
掲載ページ	p. 49-63
発行年月	1984年12月

専大北海道紀（自然）J. of Senshu Univ., Hokkaido (Nat. Sci.) 17 P. 49～63 (1984)

Soil Failure by Introducing Fluid under Pressure

— Differences of soil failure at different soil moisture contents —

Ken ARAYA, Rui GAO

流体圧送による土壌層の破壊

—— 含水比の違いによる土壌破壊の違い ——

新家　憲司・高　　鋭

要　旨

土壌層内に空気を圧送して土壌を破壊する時，土壌の含水比が異ると，全く異った破壊をするのが観察された。そこで含水比が異ると土壌中に，どのような応力が働らいて破壊するのか，有限要素法によって明らかにした。

この結果，含水比が通常（塑性限界以内）の場合は，土は圧送空気の静圧によって生ずるせん断応力によって破壊する。含水比が増加して(液性限界附近)，空気が土壌中を流れ難くなると，引張り応力が働き，土は裂断的に壊れる。この裂断形の破壊状態は，流体が液体でも，流れにくければ観察される。

せん断応力による破壊は，圧送流体を液肥として，サブソイラなどのけん引低抗力を減ずるのに応用が出来ると考えている。また引張り応力による破壊は，圧送流体を空気として，水田表面水の排水などに応用が出来ると考えている。

本報の最終の目的は，このような作業機を開発することであるが，例えば，この装置において適正なノズル口の位置，適正なチゼルの長さを知るためには，流体圧送によって土壌内にどのような応力が働らいて破壊するかを知る必要がある。

土は弾塑性体で，破壊の条件も Von Mises の降状条件に従うのが適切と思われるが，本報では，流体が土の中を流れる時の難易によって，土壌内応力がどのように違うか概略分れば良いから，近似的に土壌層を弾性体としてあつかって有限要素法で解析した。

流す流体は，簡単のため流体によって土の強度が変化しない空気とした。

Acknowledment: This research was supported in part by a National Grant-in-Aid for Scientific Research.

The author are: K. ARAYA, Professor, Agricultural Engineering Dept., Senshu University, Bibai, Hokkaido, JAPAN, and R. GAO, Engineer, Chinese Academy of Agricultural Mechanization Science, Peiking, People's Republic of CHINA.

This article was presented at the 1983 Meeting of JSAM at Ryukyu University.

I. ABSTRACT

When air under pressure was introduced into a soil layer to break it down, the nature of soil failure observed varied with the moisture content of the soil. This research was conducted to analyze differences of stress in soil induced by injecting air into the soil layer with varied moisture content by the finite element method (FEM).

When the moisture content was below the plastic limit, the soil was broken down by shearing stress produced by static pressure of the injected air.

When the moisture content was increased (close to the liquid limit), and soil showed a high resistance to air permeability, soil was disrupted by tensile stress as if it had been torn. This phenomenon was observed even if injected fluid was liquid.

II. INTRODUCTION

When air was introduced under pressure into a soil layer having low resistance to permeability, a V-shaped slip line was produced in the soil and a cavity was formed near the nozzle port as shown in Photo 2. If the soil layer had a high resistance to permeability, it was disrupted, producing a horizontal crack as shown in Photo 3. This phenemenon was observed even if injected fluid was liquid (Araya, 1980 (a)).

It might be possible to use the failure shown in Photo 2 for the draft reduction of subsoilers by injecting liquid such as liquid fertilizer. Also, it might be possible to apply the failure shown in Photo 3 for drainage in paddy fields by injecting air.

The final object of this research is to develop machines for these purposes, but it is necessary to know what kind of stress causes in soil layer to break down, in order to decide, for example, an appropriate position of the nozzle port or a proper length of the subsoiler chisel in this system.

Since soil is an elastic-plastic body, the conditions for its failure must be due to Von Mises'es yield condition (Whlie, 1960, Hyodo, 1980, Kitani, 1975(a), Young, 1977). However, assuming soil was approximately an elastic body in this paper, we analyzed stress by FEM because the purpose of the analysis was making clear the approximate differences of stress caused in the soil layer at different permeabilities.

The experiment was conducted using air which was easily handled and did not change the strength of soil by its flow.

III. RESISTANT PRESSURE PRODUCED WHEN AIR FLOWS RADIALLY IN SOIL LAYER

Previous publications (Araya, 1980(b), 1981) reported the pressure produced when injected fluid

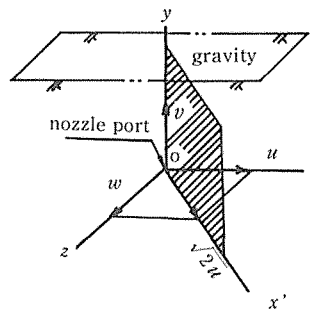

Fig. 1 Direction of velocity of flow and its resultant plane

flowed through soil spreading in three dimensions. They are summarized as follows.

When air flows radially from point O in soil layer as shown in Fig. 1, the flow pattern is symmetric for y-axis and $u=w$, $\partial p/\partial x=\partial p/\partial z$. Considering the new x'-y plane between x-axis and z-axis (45°), a flow velocity $\sqrt{2}\,u$ which is a resultant velocity of u and w is produced in this plane. Therefore, the flow pattern of air flowing radially (in three dimensions) can be expressed approximately by a two-dimensional flow in x'-y plane. The pressure produced at a nozzle port (point O) is as follows:

$$p_{inf}\,(p_{inf}+2p_0)=J\cdot\Lambda\cdot G_t\cdot g\frac{RTC_s\mu S_v^2}{9}\cdot\frac{(1-\varepsilon+\varepsilon s)}{\varepsilon^3(1-s)^3}\ln\frac{2L}{r_0} \tag{1}$$

where:

p_{inf} = gauge pressure produced at the nozzle port, Pa

p_0 = atmospheric pressure $=1.013\times10^5$, Pa

G_t = mass flow rate, kg/s

R = gas constant $=29.27$, m/°K

T = absolute temperature, °K

C_s = constant, 100 for almost all soils (Araya, 1978), —

μ = coefficient of viscosity, N·s/m²

g = gravitational acceleration $=9.8$, m/s²

S_v = surface area per unit volume of both soil particles and moisture (shows a difficulty of fluid flow in the soil, Araya, 1978), m²/m³

ε = porosity, —

s = degree of saturation, —

L = distance between nozzle port and ground surface, m

r_0 = radius of nozzle port, m

J = potential constant, l/m

$$=\ln\left[(1.078\times10^{-4}/r_0)+1.006\times10^{-2}\right] \tag{2}$$

Λ = coefficient of turbulent flow, —

$$=(Ren/20)^{0.4} \tag{3}$$

Ren = Renold's number at the nozzle port, —

$$=\frac{6G_t}{\pi r_0^2(1-\varepsilon+\varepsilon s)S_v\mu} \tag{4}$$

The coefficient of turbulent flow Λ can be calculated from equation (3) When $Ren\geqq20$ and is always 1 when $Ren<20$.

The pressure produced on each of the co-ordinates in the soil layer is as follows:

$$p_{xy}=\psi\frac{JG_tg}{2k}\ln\frac{(y-L)^2+(x'/\sqrt{2})^2}{(y+L)^2+(x'/\sqrt{2})^2} \tag{5}$$

where:

p_{xy} = static pressure produced in soil layer, Pa

$$k=\frac{18\rho g}{C_s\mu S_v^2}\cdot\frac{\varepsilon^3(1-s)^3}{(1-\varepsilon+\varepsilon s)^2},\quad \text{m/s} \tag{6}$$

ψ in equation (5) is 1 when the flow in soil is laminar flow ($Res<20$) and is more than 1, which is calculated from the following equation, when a turbulent flow ($Res\geqq20$)

$$\psi=\frac{1}{C_s}(a+b\cdot Res),\quad — \tag{7}$$

where:

a, b = constants which are individual for each soil, a function of S_v (Araya, 1978), —

Res = Renold's number in soil, —

$$= \frac{6|V|\rho}{(1-\varepsilon+\varepsilon s)S_v\mu} \tag{8}$$

$\mathbf{V}$ = resultant vector velocity of flow in x', y directions, m/s

$$= \sqrt{2u^2+v^2} \tag{9}$$

The velocity of flow in x' and y directions is respectively as follows:

$$u = -\frac{JQ}{2}\cdot\frac{x'}{(y-L)^2+(x'/\sqrt{2})^2} + \frac{JQ}{2}\cdot\frac{x'}{(y+L)^2+(x'/\sqrt{2})^2} \tag{10}$$

$$v = -JQ\cdot\frac{(y-L)}{(y-L)^2+(x'/\sqrt{2})^2} + JQ\cdot\frac{(y+L)}{(y+L)^2+(x'/\sqrt{2})^2} \tag{11}$$

where:

u, v = velocity of flow in x' and y directions, m/s

ρ = density of air (mean values of density at nozzle port and density under atmospheric pressure), kg/m³

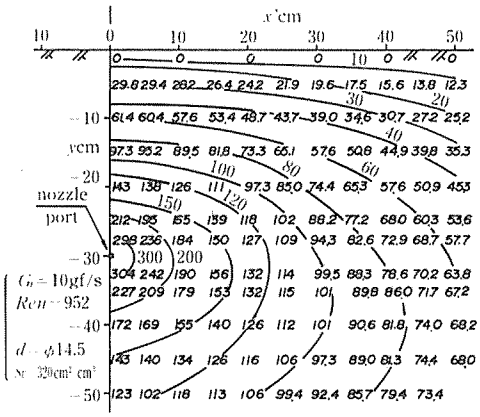

(a) produced pressure-distribution of the whole of soil layer (hPa)

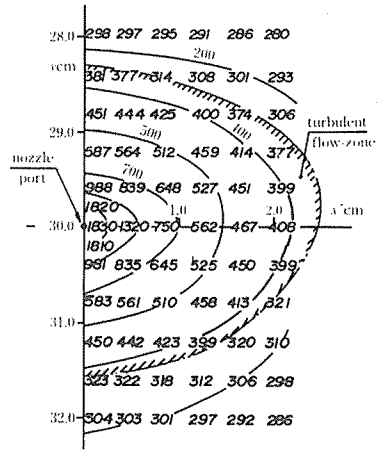

(b) pressure distribution at near part around nozzle port (hPa)

The direction of flow in $x'-y$ plane in Fig. 1 is as follows:

$$\cos\theta = \sqrt{2}\, u/|\mathbf{V}|$$

where:

θ = angle between the direction of flow and x'-axis, deg

Fig. 2 shows the pressure distribution and flow pattern calculated from the above equations as an

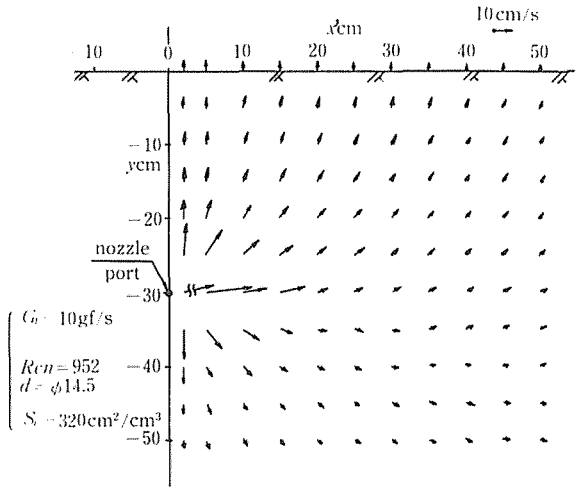

(c) flow-pattern of the whole soil layer

Fig. 2 An example of pressure-distribution and flow-pattern

example when air is introduced into clay loam layer having 15 % moisture content. The position of the nozzle port is at $L=0.3$ m from the ground surface and the flow rate of air is $G_t=0.01$ kg/s. In Fig. 2(a), the numerical values of the pressure produced at the nozzle port, i.e. $p_{inf}=1830$ hPa (from equ. (1)), relate to those of the pressure produced in soil layer (from equ. (5)) and there is no discontinuous point. Fig. 2 (b) show the pressure distribution near the nozzle port and the turbulent flow zone is shown by an egg-shaped hatched area where $Res \geqq 20$. This turbulent zone is a narrow area no more than 2 cm from the nozzle port. Fig. 2 (c) show directions of flow which show that most of injected air flows foward the ground surface.

IV. ANALYSIS BY FEM

We took a layer 1 cm thick in order to analyze the stress caused in the soil layer as shown in Fig. 3. The elements around the nozzle port were divided into smaller elements. The nozzle port was set at −30 cm from the ground surface in y direction and at 30 cm from the subsoiler standard in x direction.

We assumed that there were an infinite number of holes, 2×2 mm in side (marked "hole element" in Fig. 3), in the soil layer and loads induced by the static pressure shown in Fig. 2 acted only on these hole elements. Since the static pressure dropped drastically at any distance from the nozzle port as shown in Fig. 2, it allowed the loads to act within a zone of only 10 cm around the nozzle port. The dynamic pressure induced by velocity of flow in Fig. 2 (c) was not considered as a factor because it has been clear that the dynamic pressure had an effect of less than 1/10 of the static pressure for the soil failure (Araya, 1980 (a)).

The loads act at the four nodal points of the hole element and can be obtained from a method shown in Fig. 4. When calculating the loads caused at the hole element where pressure p_1 is working,

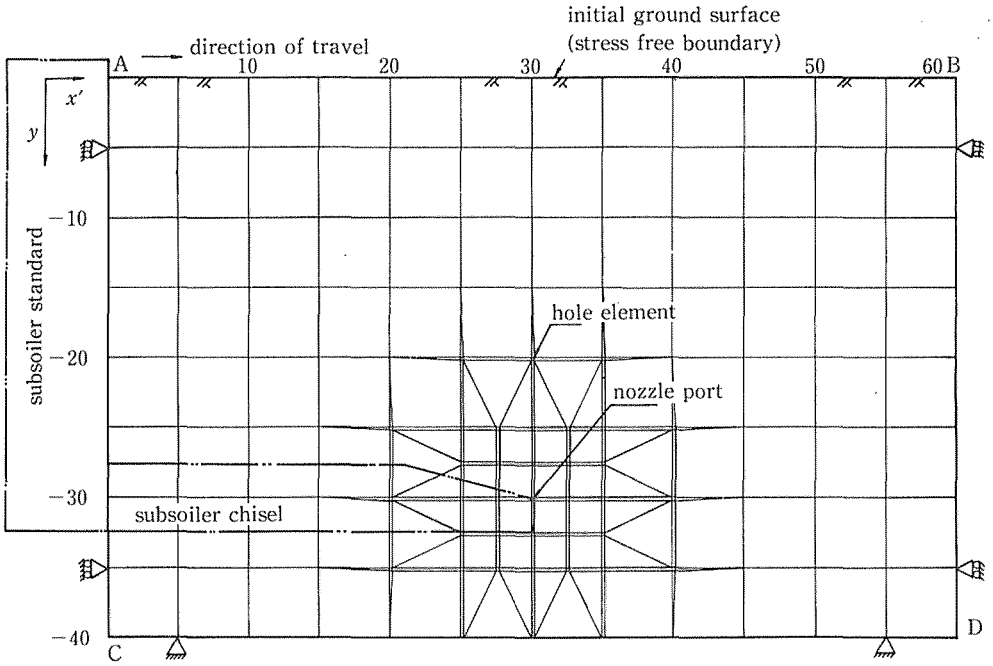

Fig. 3 Finite element mesh idealized the air injecting subsoiler-soil system

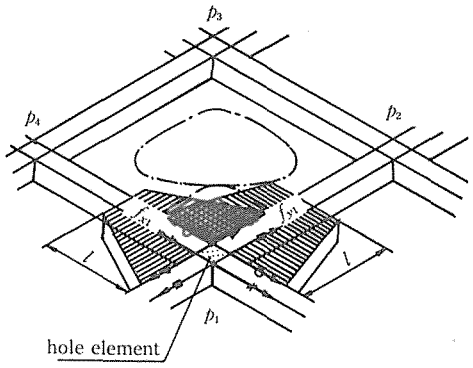

Fig. 4 How to calculate loads from static pressure

we consider three neighboring hole elements as having an effect on p_1. If pressure p_1, p_2, p_3 and p_4 work at each hole, and it is assumed that soil layers having 1 mm thick are piled up over middle point of a hole element and a neighboring hole element (distance l), the loads in x and y directions are as follow:

$$f_{x1}=\frac{p_{12}+p_1}{2}l\times\frac{l}{10^{-3}}=500(p_1+p_{12})l^2 \tag{13}$$

$$f_{y1}=\frac{p_{14}+p_1}{2}l\times\frac{l}{10^{-3}}=500(p_1+p_{14})l^2 \tag{14}$$

where:

f_{x1}, f_{y1} = loads in x and y directions at the hole element where pressure p_1 works, N

p_{12}, p_{14} = mean value of pressure p_1 and p_2 , Pa, mean value of pressure p_1 and p_4, Pa

$2l$ = distance between the two hole elements under consideration, m

In Fig. 3, when we analyzed the stress in the soil layer produced when air was injected when the subsoiler is stationary, we made x directions of AC plane and BD plane fixed (horizontal displacement = 0) and their y directions free. When the subsoiler proceeded injecting air, we made these all planes free. In any case, AB plane was always free and CD plane was always fixed (vertical and horizonal displacement = 0).

When the subsoiler proceeded, we gave both the nodal points on AC plane which the subsoiler standard touched and the nodal points at the nozzle port (the tip of the subsoiler chisel) specified displacement in x-direction respectively.

V. EXPERIMENTATION

Laboratory tests were conducted in a movable soil bin shown in Photo 1. One side of this soil

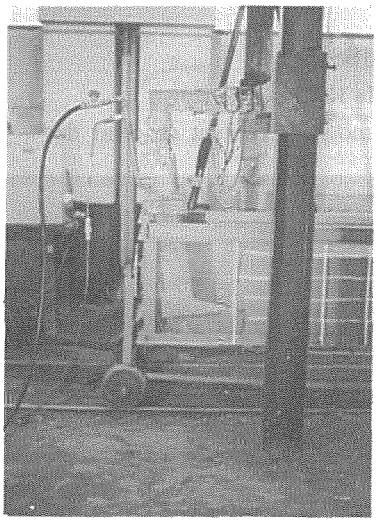

Photo 1 Air injecting subsoiler in soil bin

bin was made of a transparent acryl resin through which the nature of soil failure could be observed. At the same time, the pressure produced at nozzle port was measured by a pressure transducer.

The soil in this study was clay loam with little organic matter. The moisture content was kept at 2 levels i. e. 15 % and 30 %. The plastic limit of this soil was 23.7 % and the liquid limit was 34.6 %. All moisture contents are expressed on a dry weight basis. Soil preparation was accomplished by compacting the soil into layers 10 cm thick. The soil hardness was kept at 14 mm on the Yamanaka hardness tester scale.

Fig. 5 shows the strength characteristics of this soil. The shearing strength was measured by the

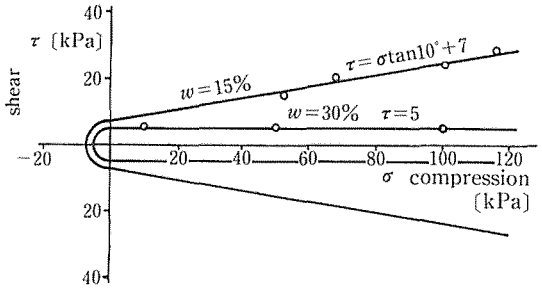

Fig. 5 Strength of studied soil at different moisture content

direct shear test and the tensile strength was measured by the radial compression test (Kawamoto, 1968). Table 1 shows the physical properties at the two different moisture contents.

Table 1 Soil strength properties at different moisture content (clay loam, 14mm soil hardness on Yamanaka hardness tester scale)

moisture content w	Young's modulas E(MPa)	poisson ratio ν (—)	S_v (1/m)	a	b
15%	1.28	0.25	3.2×10^4	84	1.7
30%	0.15	0.25	8×10^5	102	3.6

VI. RESULT AND DISCUSSION

1. When Soil Moisture Content Is 15%.

Fields generally have this moisture content on clear days. Photo 2 shows the nature of soil

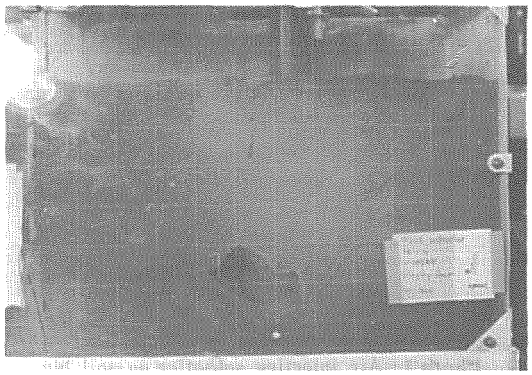

(a) subsoiler is stationary

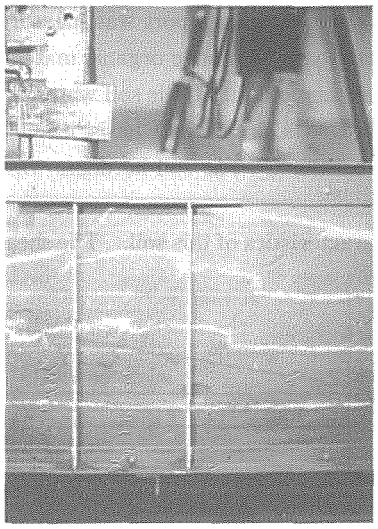

(b) Subsoiler is proceeding to the right

Photo 2 The nature of soil failure of clay loam having 15% moisture content (G_t =10g/s)

failure induced when air of 10 g/s was injected. Photo 2 (a) shows the phenomenon observed when the subsoiler was stationary. A cavity was formed around the nozzle port and a V-shape slip line that reached the ground surface was produced. Photo 2 (b) shows the phenomenon observed when the subsoiler was moving to the right and a cavity was formed around the nozzle port and the slip line reaching the ground surface, along which the soil was shifted upward cosiderably, was produced.

Figs. 7 (a), (b) show an analysis of stress fields corresponding to Photos 2 (a), (b). Fig. 6 shows loads (block line) corresponding to Photo 2 (a). These loads were calculated from equations (13), (14) by using the value of the pressure shown in Fig. 2.

In Fig. 7 (a), only compressive stress acts on the elements around the nozzle port and this means all the soil is broken down solely by shearing stress. Kitani (1975 (b)) reported that soil failure by tensile stress could be produced by introducing air. But such phenomenon can never be expected.

Drawing Mohr envelopes on Fig. 5 by using these produced compressive stress values shown in Fig. 7 (a), the failure zone which may be broken down by the shearing stress is shown by the hatched part. This zone takes a symmetrical V for the nozzle port and is in close agreement with the nature of failure shown in Photo 2 (a).

Fig. 7 (b) shows the stress fields induced when the subsoiler gave the soil specified displacement of 0.5 cm. The failure zone is shown by hatched area from the physical properties in Fig. 5. The darker hatched area shows the zone which may be broken down by tensile stress. The failure at the area 10 cm from the bottom (CD plane) was not taken into consideration because this area has a

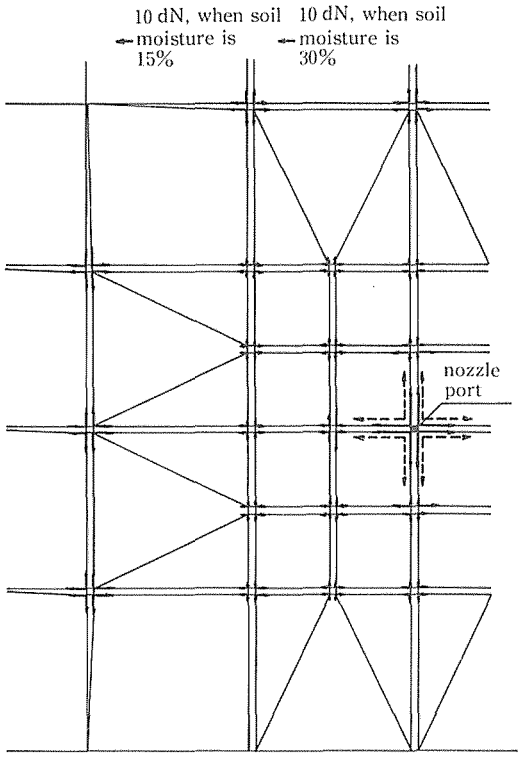

Fig. 6 Loads at each hole calculated from pressure distribution in Fig. 2

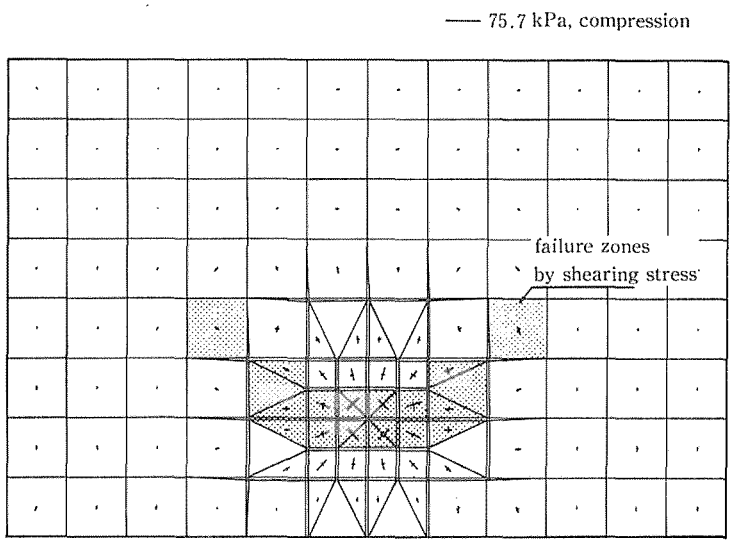

(a) When subsoiler is stationary

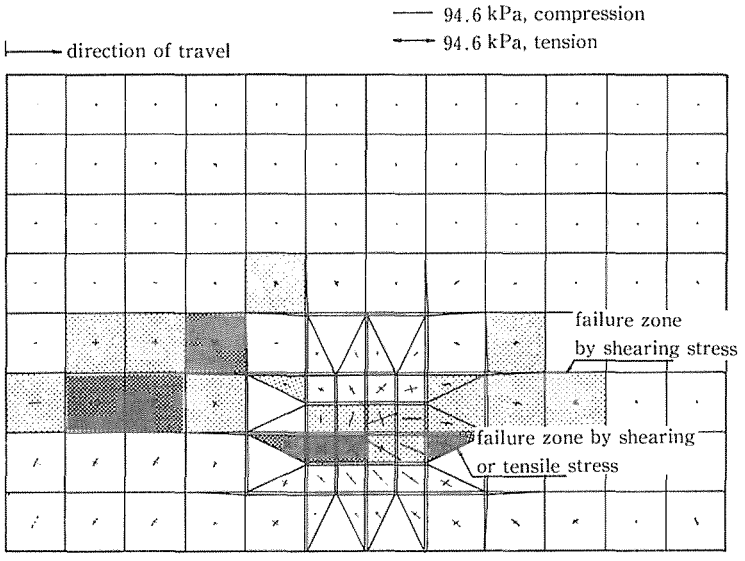

(b) After 0.5 cm subsoiler movement

Fig. 7 Stress fields induced when air of 10 g/s is injected into soil having 15% moisture content

restricted effect by FEM analysis, and besides it was made clear from the experiment shown in Photo 2 (b) that the soil layer within 10 cm from the bottom had no change.

In Fig. 7 (b), another slip line is produced by moving the subsoiler standard. This slip line does not reach the slip line induced by air injection but is independent, when the displacement is 0.5 cm or less.

Since the nodal points at the nozzle port are also moved 0.5 cm to the right, as shown in Fig. 7 (b), the failure zone around the nozzle port is shifted in the direction of travel (to the right) as contrasted

with that in Fig. 7 (a).

If the slip line induced by moving the subsoiler standard is not above the slip line induced by injecting air, a larger draft reduction could be expected because a greater volume of soil is broken down. Consequently the nozzle port should be separate from the subsoiler standard, the chisel should be as long as strength permits, and the nozzle port should be at the tip of the chisel.

In the experiment shown in Photo 2 (b), the cavity formed by injecting air was about 10 cm from the tip of the chisel when the subsoiler was moving. This may be due to the fact that injected air flows out to the slip line induced by moving the subsoiler standard. If air flows out to the atmosphere, air under pressure does not effectively produce soil failure. Consequently the nozzle port should be separate from the subsoiler standard for this reason, too.

2. When Soil Moisture Content Is 30%.

Soil after it rains or soil in paddy fields has such moisture content. Photo 3 shows the nature of soil failure induced when air of 10 g/s was injected into this soil. Photo 3 (a) was when the subsoiler was stationary and Photo 3 (b) was when the subsoiler was moving. In both cases, big horizontal cracks

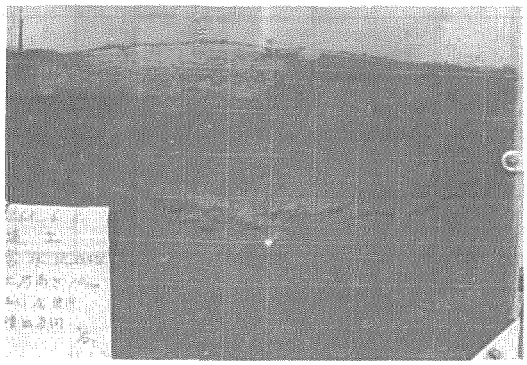

(a) subsoiler is stationary

(b) Subsoiler is proceeding to the right

Photo 3 The nature of soil failure of clay loam having 30% moisture content (G_t=10g/s)

were produced in the soil layer.

Fig. 8 shows the stress fields of this soil corresponding to Photo 3. Since soil had a high resistance to permeability, we had the load act at only four nodal points of nozzle port as shown in Fig. 6 (dotted line).

Fig. 8 (a) shows that tensile stress acts at each element in this case. From the strength properties in Fig. 5, the failure zone is a symmetrical hatched part for the nozzle port and this zone has a possibility

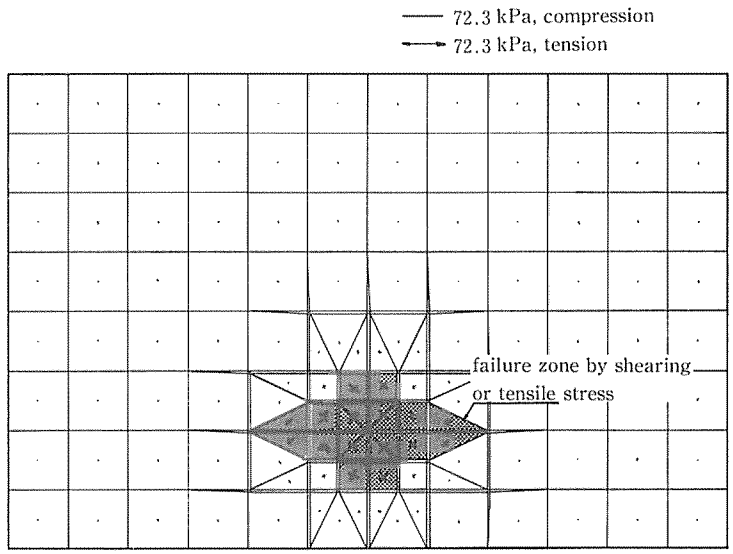

(a) When subsoiler is stationary

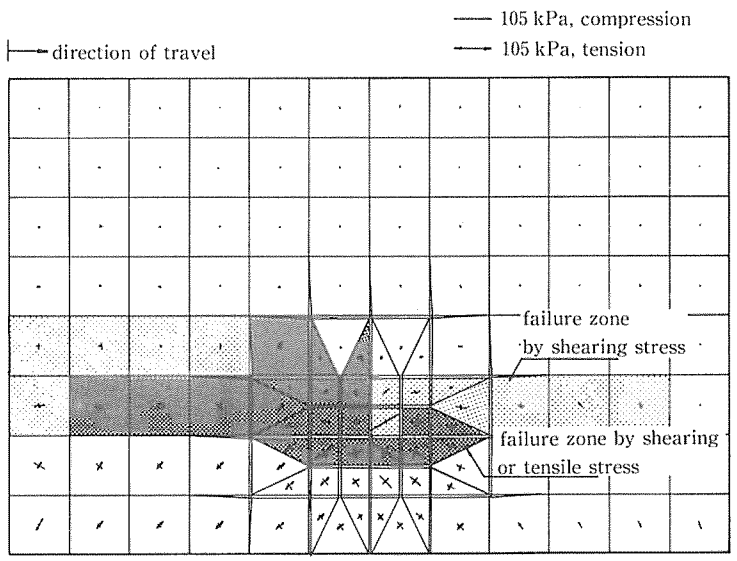

(b) After 5 cm subsoiler movement

Fig. 8 Stress fields induced when air of 10 g/s is injected into soil having 30% moisture content

of failure by both the tensile stress and the shearing stress. Fig. 8 (a) does not have the V-shaped slip line shown in Fig. 7 (a).

However Fig. 8 (a) does not make clear that cracks are produced horizontally as shown Photo 3 (a). This may be due to the fact that element around the nozzle port is too rough. If a finer mesh was used and the stress of the semi-infinite plate with a hole in which pressure is working was analyzed, it could be made clearer that cracks are produced horizontally by the powerful induced horizontal tensile stress. Fig. 8 (b) shows the field induced when the subsoiler moved 5 cm in x-direction. A greater number of those elements in contact with the lower part of the subsoiler chisel were broken down by shearing stress. However the slip line reaching the ground surface as shown in Fig. 7 (b) did not occur. This is in agreement with the experiment shown in Photo 3 (b).

In soil having 30% moisture content, if the nozzle port was close to the subsoiler standard, the horizontally produced cracks reached the subsoiler path easily and the injected air farely distrupted the soil but leaked to the atmosphere. Therefore the nozzle port should be as far from the subsoiler standard as possible in this case, too.

Fig. 9 shows the soil deformation which corresponds to Fig. 8 (b). The elements around the nozzle port are deformed considerably above and below, and the production of horizontal cracks can be estimated from this figure.

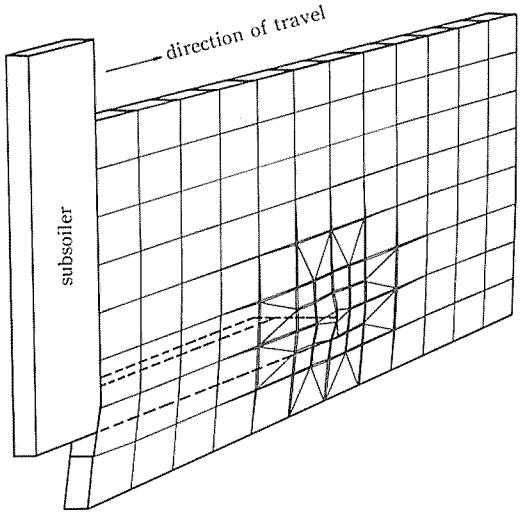

Fig. 9 Displacement field after 5 cm subsoiler movement when air of 10 g/s is injected into soil having 30% moisture content

VII. CONCLUSIONS

When air under pressure was introduced into a soil layer to break it down, the nature of soil failure observed varied with the moisture content of the soil. This research was conducted to analyze differences of stress in soil induced by injecting air into the soil layer with varied moisture content by the finite element method (FEM).

When air was introduced under pressure into a soil layer having low resistance to permeability, a V-shaped slip line was produced in the soil and a cavity was formed near the nozzle port as shown in

Photo 2. If the soil layer had a high resistance to permeability, it was disrupted, producing a horizontal crack as shown in Photo 3. This phenomenon was observed even if injected fluid was liquid.

It might be possible to use the failure shown in Photo 2 for the draft reduction of subsoilers by injecting liquid such as liquid fertilizer. Also, it might be possible to apply the failure shown in Photo 3 for drainage in paddy fields by injecting air.

The final object of this research is to develop machines for these purposes, but it is necessary to know what kind of stress causes in soil layer to break down, in order to decide, for example, an appropriate position of the nozzle port or a proper length of the subsoiler chisel in this system.

Since soil is an elastic-plastic body, the conditions for its failure must be due to Von Mises'es yield condition. However, assuming soil was approximately an elastic body in this paper, we analysed stress by FEM because the purpose of the analysis was making clear the approximate differences of stress caused in the soil layer at different permeabilities. Main results were as follows:

1. Fig. 2 shows the pressure distribution and the flow pattern when air is introduced into clay loam layer having 15% moisture content. Fig. 2 (b) shows the pressure distribution near the nozzle port and the turbulent flow zone is shown by an egg-shaped hatched area where $Res \geqq 20$. This turbulent zone is a narrow area no more than 2 cm from the nozzle port. Fig. 2 (c) show directions of flow which show that most of injected air flows toward the ground surface.

2. The soil in this study was clay loam with little organic matter. When air was introduced under pressure into this soil layer having 15% moisture content (corresponding to the condition on clear days), a V-shaped slip line reaching the ground surface was produced in the soil and a cavity was formed near the nozzle port as thown in Photo 2.

3. Fig. 7 (a), (b) show an analysis of stress fields analyzed by FEM corresponding to Photos 2 (a), (b). In Fig. 7, only compressive stress acts on the elements around the nozzle port and this means all the soil is broken down solely by shearing stress. The failure by tensile stress can not never be expected.

4. Photo 3 shows the nature of soil failure induced when air was injected into the soil having 30% moisture content (corresponding to the condition on rainy days or in paddy fields). Big horizontal cracks were produced in the soil layer.

5. Fig. 8 shows the stress fields of this soil analyzed by FEM corresponding to Photo 3. Fig. 8 (a) shows that tensile stress acts at each element in this case. From the strength properties in Fig. 5, the failure zone is a symmetrical hatched part for the nozzle port and this zone has a possibility of failure by both the tensile stress and the shearing stress.

6. If the slip line induced by moving the subsoiler standard is not above the slip line induced by injecting air, a larger draft reduction could be expected because a greater volume of soil is broken down. Consequently the nozzle port should be separate from the subsoiler standard, the chisel should be as long as strength permits, and the nozzle port should be at the tip of the chisel.

7. If air flows out to the atmosphere, air under pressure does not effectively produce soil failure. Consequently the nozzle port should be separate from the subsoiler standard for this reason, too.

References

1) Araya Ken. 1978. Fluid Friction Resistance of Soils. J. of JSAM. Hokkaido. 19
2) Araya Ken et al. 1980 (a). Pressure Produced and Breakdown of Soil when Fluid is Introduced under Pressure into Soil Layer. J. of JSAM. Hokkaido. 21
3) Araya Ken. 1980 (b). Pressure Produced when Fluid is Introduced under Pressure into a Soil

Layer (II). J. of JSAM. 42 (3)

4) Araya Ken. 1981. Flow Pattern and Pressure Distribution in Soil Layer. J. of Senshu Univ. Hokkaido. 14
5) Kawamoto T. 1968. Applied Elasticity. Kyoritsu Press.
6) Hyodo Kazuya et al. 1980. Studies on Soil Cutting by a Blade. Proceedings of the First Conference on Terramechanics.
7) Kitani Osamu. 1975 (a). Analysis of Stress caused in Furrow by FEM. J. of JSAM. 37 (2)
8) Kitani Osamu. 1975 (b). Basic Studies on Pneumatic Tillage. J. of Mie Univ. 48
9) Wylie C. R. 1960. Advanced Finite Element Method. Brain Press.
10) Young R. N. and Hanna. A. W. 1977. Finite Element Analysis of Plane Soil Cutting. J. of Terra. 14 (3)